Molecular Crystals and Liquid Crystals
Publication details, including instructions for authors and subscription information:
http://www.tandfonline.com/loi/gmcl16

The Role of Image Forces at Organic Crystal/Elecrtrode Interfaces

M. E. Michel-beyerle [a], W. Harengel [a], R. Haberkorn [b] & J. Kinder [c]
[a] Institut für Physikalische Chemie, Technische Universität, München
[b] Physik-Department, Technische Universität, München
[c] Gesellschaft für Strahlenforschung Abt. Kohärente Optik, Neuherberg bei, München, Germany
Version of record first published: 29 Aug 2007.

To cite this article: M. E. Michel-beyerle , W. Harengel , R. Haberkorn & J. Kinder (1974): The Role of Image Forces at Organic Crystal/Elecrtrode Interfaces, Molecular Crystals and Liquid Crystals, 25:3-4, 323-338

To link to this article: http://dx.doi.org/10.1080/15421407408082810

Mol. Cryst. Liq. Cryst., 1974, Vol. 25, pp. 323-338

Printed in Dordrecht, Holland

The Role of Image Forces at Organic Crystal/Electrode Interfaces

M. E. MICHEL-BEYERLE and W. HARENGEL

Institut für Physikalische Chemie,
Technische Universität, München

R. HABERKORN

Physik-Department, Technische Universität, München

and

J. KINDER

Gesellschaft für Strahlenforschung
Abt. Kohärente Optik,
Neuherberg bei München, Germany

(Received April 23, 1973)

Photocurrents in anthracene crystals originating from exciton decay at silver and aqueous electrolyte electrodes were measured in steady state as well as in space-charge-free transients. In both experiments metal and electrolyte electrodes show markedly different behaviour at field strengths in the range $10^3 - 10^5$ V/cm. This is attributed to the influence of the image force on charge separation at metal electrodes contrary to electrolyte contacts where the image force is negligible due to the slow orientation polarization of water as compared to the hopping frequency of injected charge carriers. From the steady state current-voltage plot the surface recombination rate of holes at the silver electrode is estimated to be of the order of 10^3 cm/sec.

INTRODUCTION

Electronic conduction in organic molecular crystals with weak electronic interaction between the molecules (~ 200 cm^{-1}) may originate from unipolar charge carrier injection at the crystal surface, either in thermodynamic equilibrium with

an electrode of suitable Fermi energy, or, as will be exclusively discussed in this paper, during non-equilibrium photochemical reactions. In the latter case, exitons, generated by absorption of light in the crystal, may diffuse to the crystal surface and undergo electron transfer reactions with electron-donating or electron-accepting species. Charge carriers which migrate into the bulk of the crystal under the influence of an externally applied electric field have to overcome a potential barrier at the crystal surface by diffusion. This potential barrier arises from image forces, from Coulomb interaction with localized or slowly mobile counter charges, from the space charges and from the external electric field. Since at low field strengths space charge effects are more important than image and Coulomb forces, investigation of the latter should be restricted to field strengths, where space charges are negligible to a first approximation. Furthermore, an important feature in the non-equilibrium case consists in the irreversible loss of charge carrieres by recombination with the electrode.

In an earlier paper[1] the phenomenology of the current-voltage (j-U) plot of photocurrents was discussed for electrodes with comparable rate constants for the primary charge carrier generation step but different electrostatic properties. For metals as electrodes no saturation currents were found up to a field strength of 7.10^4 V/cm, due to image forces and surface recombination. However, the phase boundary molecular crystal/aqueous electrolyte exhibited saturation currents at field strengths far below 10^5 V/cm. In this case image forces can be neglected due to the slow orientation polarization of water molecules with respect to the hopping frequency of the injected charge carriers. Coulomb forces arising from slowly mobile or localized counter charges are shown to be effectively screened by water as a result of its relatively higher static dielectric constant compared to that of the crystal.[1,15]

The often discussed possibility[2] that—in analogy to metal-electrolyte interfaces[3]—electric double layers reduce the potential barrier at the phase boundary crystal/aqueous electrolyte does not apply to solids with the properties of molecular crystals.[13]

In this paper, the interaction of excitons with redox systems in aqueous electrolytes as electrodes will be compared with that occurring at a metal electrode of comparable Fermi energy (Figure 1). A possible determination of the rate constant of surface recombination of charge carriers is discussed.

EXPERIMENTAL DETAILS

Anthracene crystals (triplet exciton lifetime ~15 msec) were grown from purified material (kindly placed at our disposal by Dr. Karl, Kristall-Labor Stuttgart) and cleaved perpendicularly to the ab-plane (Figure 2) into identical moieties. After purification of the surface by high vacuum treatment

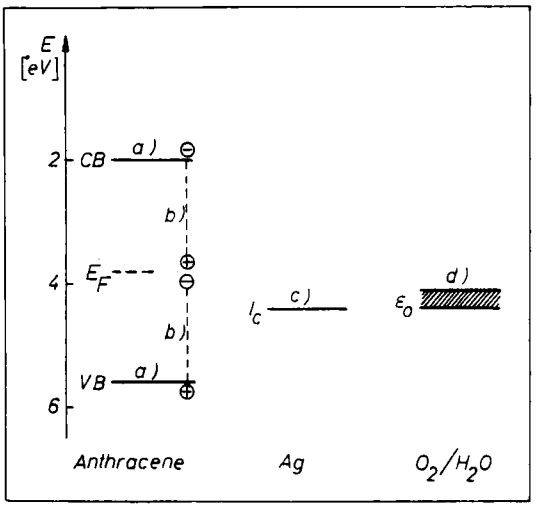

FIGURE 1 Energy level diagram: (a) Crystal data of anthracene are taken from Refs. 8,9, work function I_c = 5.65 eV, band gap 3.8 eV. (b) For simplicity triplet exciton energy is indicated in the one-particle energy spectrum. (c) Work function of silver films, I_c = 4.44 eV after R. Suhrmann and G. Wedler, *Z. Angew. Physik* 14, 70 (1962). (d) Conversion of standard redox potential versus normal hydrogen electrode (NHE) into the absolute energy scale after F. Lohmann, *Z. Naturf.* **22a**, 843 (1967). The tolerance is given for the uncertainty as to the reversible one-electron redox potential of molecular oxygen in aqueous electrolyte.

($\sim 10^{-5}$ torr) at room temperature, silver has been evaporated onto one of the two parts at low temperature (77°K). The crystals were stored under nitrogen atmosphere in the dark.

Steady state photocurrents were measured in the conventional way. Excitation source: 900 W XBO (OSRAM) in combination with a Bausch and Lomb High Intensity Monochromator 511 UB (band width 5 nm) and a Nicol prism. Electric fields were applied via a high voltage supply (KEITHLEY 246); currents were measured by a KEITHLEY 610c-electrometer. The illuminated face of the crystal (with the light being polarized parallel to the crystallographic *b*-axis) was always negatively biased. Under this condition and the wavelength of excitation (λ = 420 nm, crystal thickness 80 μ) the photocurrent originated from the injection of holes by interaction of triplet exciton with an electron acceptor (molecular oxygen, silver) at the non-illuminated face of the crystal. The measurement of photocurrents at high field strenght always anteceded the plot of the lower part of the current-voltage curve.

The experimental arrangement (Figure 2) for the measurement of SCF-transients was conventional[4] with the exception of the light source: a frequency

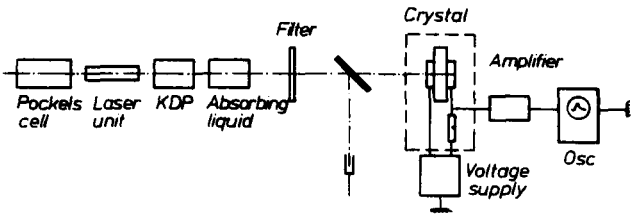

FIGURE 2 Measuring assembly

doubled ruby laser flash at the wavelength of 347 nm with a half intensity width of 15 nsec. Crystals, sample holder and electrodes were identical with those in stationary photocurrents, except for hole injection originating from the illuminated face of the crystal. The signal was traced by a wide band amplifier KEITHLEY 104 and a fast oscilloscope TEKTRONIX 585A. The rise time of the circuit including the crystal was about 50 nsec, which is definitely shorter than the rise times in the SCF-transients. The photon density impinging on the crystal surface was in the range of 10^{12} photons/cm^2, as measured with a black body absorber.

RESULTS AND DISCUSSION

Steady state photocurrents

Comparison of the two current-field strength plots in Figure 3 (using identical half-portions of the crystal) shows that at field strengths $< 10^5$ V/cm exciton interaction with a metal electrode is leading to a significantly lower photocurrent than that obtained with an aqueous redox system, whereas in the saturation current region at $E > 10^5$ V/cm the photocurrent originating from exciton decay at the metal electrode certainly exceeds that measured with the electrolytic contact. This difference will be attributed to the action of image forces at the interface crystal/metal, which obviously can be neglected at the crystal/aqueous electrolyte phase boundary.

Under the condition of excitation in the tail of the long wavelength ($S_o \rightarrow S_1$) transition, with the illuminated electrode being negatively biased, the generation of holes results from the reaction of triplet excitons either with molecular oxygen in aqueous solution (A) or with a silver film (B).

At field strengths below 10^3 V/cm the current A is shown to be space-charge-limited (SCL), $j \sim E^n$ where $n = 2$ indicates shallow trapping. At $E > 5.10^3$ V/cm the current A approaches saturation, whereas at 10^3 V/cm $< E < 5.10^4$ V/cm the slope of the j-E plot B is in the range of unity

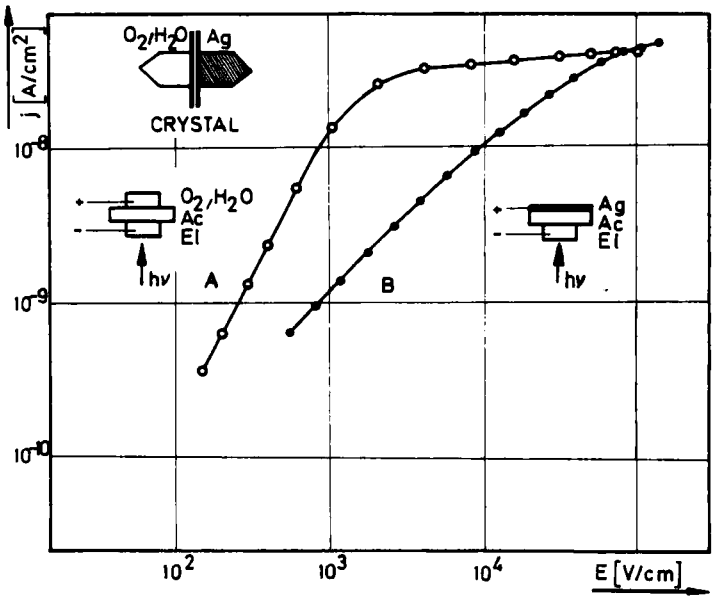

FIGURE 3 Injection of holes into anthracene crystals by striplet exciton surface reactions.
Curve A: aqueous electrode ($\sim 10^{-3}$ M O_2 as electron acceptor).
Curve B: silver film
Triplet exciton densities in A and B are equal. No hole injection in the dark to a measurable extent, neither with electrode A nor B.

($n = 0.8 - 1.1$). Obviously, the free charge carrier density in B is insufficient for space charge limitation in the range of field strengths depicted in Figure 3.

An increase of the local trap density in the vicinity of the surface due to possible damage during deposition of the metal film could not explain the j–E plot B since extremely high trap densities ($10^{12} - 10^{13}$ per cm^2) would be required. This should certainly inhibit any deflection into saturation in the high field region contrary to the experiment. Moreover, when a silver coated Mylar sheet was used as metallic electrode instead of the evaporated silver film, neither a change in the steady state j–E plot B nor in the shape of the transients (to be discussed below) was observed.

Referring to the weak electronic interaction between molecules in anthracene crystals, the injection processes will be formulated as photochemical electron transfer reactions, the energy of the conducting crystal states being roughly approximated by that of the radical ions. Injection of holes in the cases described above can be understood to occurr according to

$$^3Ac_O^* + O_2 \xrightarrow{k_1} Ac_O^+/O_2^- \tag{1}$$

and

$$^3Ac_O^*/Ag \longrightarrow Ac_O^+/Ag^- \tag{2}$$

where $^3Ac_O^*$ represents triplet excitons and Ac_O^+ holes, both at the distance $x = 0$ from the surface. Upon application of an electric field, these charge carriers may migrate into the bulk of the crystal by diffusion and drift or may recombine at the surface. We assume that a potential barrier (Figure 4) impedes the transport of carriers into the interior of the solid. This barrier is thought to exhibit its maximum value U_m in a distance x_m from the surface and arises from the superposition of the external field and the image forces. At field strenghts sufficiently high to leave the SCL-region, the photocurrent j is given by

$$j = I\frac{E}{E + \tilde{E}} \tag{3}$$

where I denotes the generation rate of charge carriers, E the external electric field and $\tilde{E} = \nu S/\mu$. In the latter term ν is the rate constant of surface recombination reactions, μ the drift mobility of injected carriers and S is a field dependent factor (see Appendix) which describes the decrease of image forces under the influence of the external field. For $E < E_i$, E_i being the field strength of the image charge, $S \to \exp(eU_i/kT)$. U_i is the depth of the image potential well. For $E \gg E_i$ follows $S \to 1$. The dependence of $\tilde{E}$ on the external field E (i.e. the field

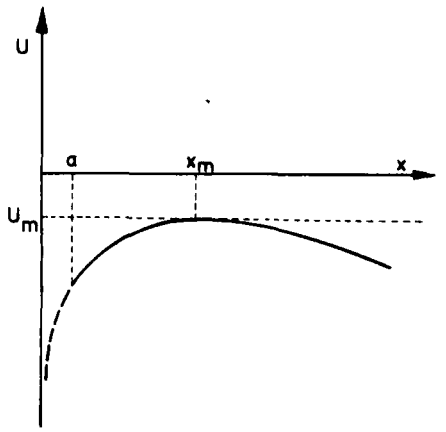

FIGURE 4 Electrostatic potential of holes vs. distance inside the crystsl from electrode. a = lattice parameter in c'-axis (~ 10 Å)

dependence of the potential maximum U_m in Figure 3) can be analyzed by plotting $1/j$ versus $1/E$, according to Eq. (4):

$$j^{-1} = I^{-1} + (I^{-1}\widetilde{E})\,E^{-1} \tag{4}$$

For low field strengths ($E < E_i$) a straight line is obtained, characterized by the slope

$$\frac{\nu}{\mu I}\exp(eU_i/kT)$$

For high fields a linear plot with a smaller slope $\nu/\mu I$ results. From Figure 5 can be concluded that for the photoinjection of holes via reaction (2), one is able to observe the beginning of the decrease of the image forces at the highest field strengths applied. In order to evaluate the surface recombination velocity ν from the slope E/I, the image potential U_i has to be estimated, since the field region $E > E_i$ was not accessible in the experiment. We assume a minimum distance between charge and surface of 10 Å, corresponding to one lattice parameter in c', which is consistent with the observation that decrease of image forces is beginning at fields $E \sim 10^5$ V/cm.With a dielectric constant $\epsilon \sim 4$ and a microscopic drift mobility of holes in anthracene of 1 cm²/V sec

$$\nu \sim 10^3 \text{cm/sec}$$

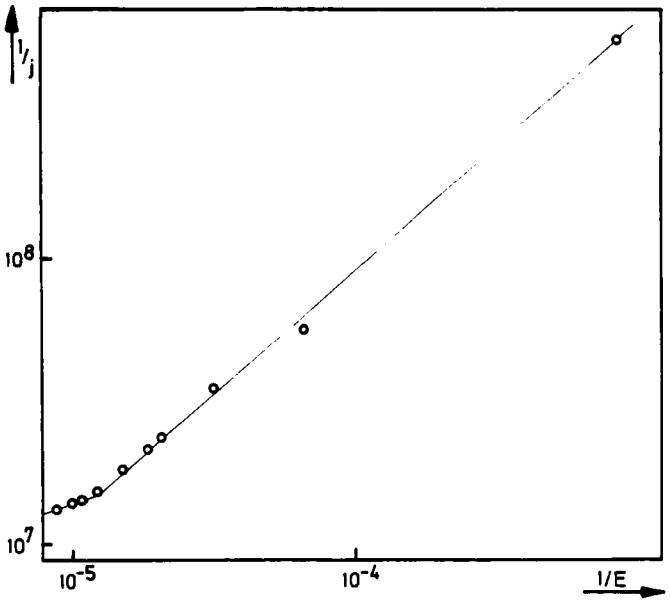

FIGURE 5 Inverse plot of curve B from Figure 3

follows for the surface recombination constant of holes at the anthracene/silver interface. The low value of ν as compared to the thermal velocity of charge carriers in anthracene ($\nu_{th} \sim 10^6$ cm/sec) could possibly reflect the low density of states in the metal as compared to that of the anthracene crystal.

In earlier work[7] the surface recombination rate between holes and a silver electrode at the *ab*-face of an anthracene crystal has been determined to be in the range of 10^2 cm/sec. This value was obtained from the falloff of charge carrier density as measured by delayed application of the electric field following flash excitation of the crystal ($\lambda = 400$ nm). It was assumed that the transport of carriers into the crystal bulk occurred exclusively by diffusion what implies that the electric field in the surface region did not exceed 10^2 V/cm. The influence of image forces, space charge and trapping was not considered. Since, however, the image force between charge carriers and a metal electrode exceeds by far 10^2 V/cm, the measured time constant for the charge carrier decay of the order of μsec should rather be attributed to detrapping of carriers than to the time constant of their surface recombination.

For an aqueous electrode (A in Figure 3) only an upper boundary for the recombination rate constant can be given, since the photocurrent enters rather abruptly the saturation current region. In accordance with our earlier paper, we conclude that at the interface anthracene crystal/aqueous electrolyte image forces can be neglected as a consequence of the high hopping frequency of charge carriers inside the crystal as compared to the time constant of the orientation polarization of water molecules.

Furthermore it is evident that the value of the saturation currents obtained with the two electron acceptors (O_2 in aqueous solution and an Ag film) is of at least the same order of manitude. This is consistent with the high rate constant k_1[5] measured for the triplet exciton/$O_2(H_2O)$ electron transfer reaction and shows at the same time that the interaction between triplet excitons and a metal film can favour electron transfer in preference to other quenching processes feasible.

Space-charge-free transients

From the analysis of the steady state current-voltage plot with silver as injecting electrode (Figure 3B) it can be concluded that at field strengths of 10^4 V/cm image forces are fully efficient. Consequently, in the analogous space-charge-free (SCF) transients as well the charge carrier flux from the surface into the crystal bulk should be governed by the diffusion flux against the image forces, whereas with aqueous electrodes the current at 10^4 V/cm is already completely determined by the drift of carriers in the external field. The onset characteristic of SCF-transients reflect the kinetics of free charge carrier generation in absence of *RC*-distortion. Thus, the question arises whether the diffusion of charge carriers

out of the image potential barrier could be mirrored in a time dependent current rise when metal electrodes are applied.

Provided that short-lived singlet excitons, generated by a nanosecond laser flash, contribute dominantly to the current, a definite charge carrier density close to the crystal surface will be established during the excitons' lifetime ($\sim 10^{-8}$sec). As follows from the steady state j–E plot (Figure 3B) at 10^4V/cm a major fraction of the primarily injected carriers recombines at the surface, whereas only a minor portion surmounts the image force barrier thermally, thus contributing to the current. Assuming a surface recombination rate of 10^3 cm/sec–as estimated above from the steady state j-E plot (Figure 3B)–and a spatial distribution of the charge carrier cloud within 2-3 lattice parameters along the crystallographic c'-axis, the resulting lifetime of free charge carriers in the image force potential barrier would be less than 10^{-9} sec. Thus the current

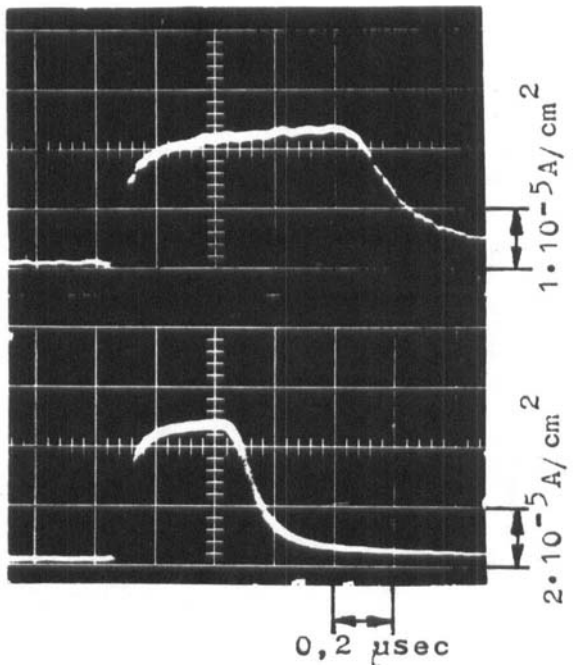

FIGURE 6 SCF-transients in anthracene crystal. Injecting electrode: O_2 (H_2O). Excitation: frequency doubled ruby laser, 347 nm, // b. Photon density: 10^{12}photons/cm^2.15 nsec. Upper trace: 6.10^3 V/cm; lower trace: $1{,}2 \cdot 10^4$V/cm, illuminated crystal face being positively biased. Crystal thickness: 40 μ.

rise characteristic of SCF-transients cannot be determined by the diffusion of free carriers. This holds even for the extreme case of dominant singlet exciton contribution to the current and a surface quenching rate of excitons exceeding their diffusion velocity. We conclude that a medium field strengths e.g. in the linear region of the j–E plot of Figure 3B the ratio of the steady state photocurrents obtained with metal and aqueous electrodes should also be observed in the current plateaus of the corresponding SCF-transients. However, this is only true as long as the relative contributions of singlet and triplet excitons to the photocurrent are the same under steady state and transients conditions.

Figure 6 and 7 compare the SCF-transients measured under identical conditions with respect to the exciting wavelength, the intensity and the electric field strength. The electron acceptors are again the prototypes used in the j–E plots of Figure 3. Short laser pulses seem to be the ideal experimental tool since the duration of the light flash is certainly short as compared to the onset of the current pulse.

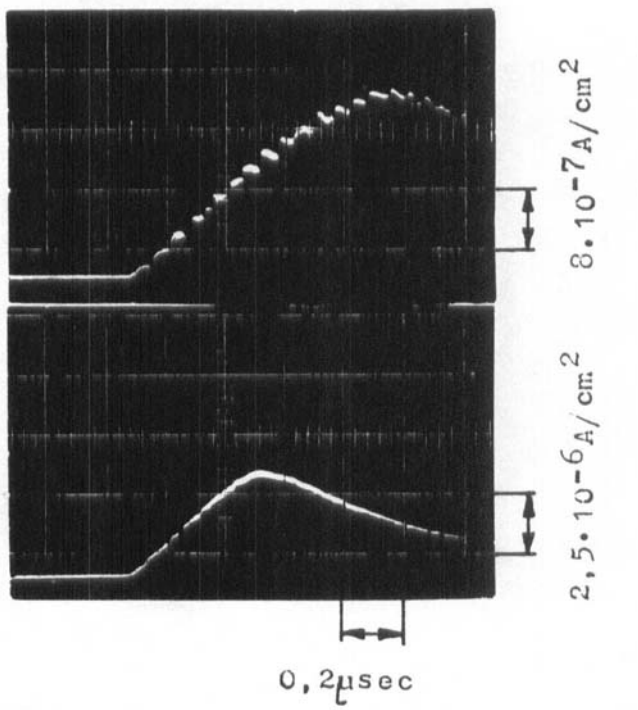

FIGURE 7 SCF-transients in anthracene crystal. Injecting electrode: silver film. Excitation, photon density, crystal thickness, strength and direction of the electric field as in Figure 6.

In both cases the voltage and the intensity dependence of the maximum current are linear as to be expected for SCF-transients. Both pulses in Figure 6 and 7 yield the drift mobility for holes $\mu = 0.65$ cm^2/V.sec in agreement with the mobility data in the literature[8]. The approximately constant charge transferred in the case of aqueous electrolyte with increasing field strength is consistent with the saturation behaviour of the steady state photocurrents at these field strengths. On the other hand, the proportional rise of the total charge with the electric field strength when silver electrodes are applied corresponds again to the linear j–E plot in Figure 3B.

The ratio of singlet/triplet excitons, $R_{S/T}$, diffusing along the c'-direction to the crystal surface can be roughly estimated for the absorption constant $\epsilon_{347\,nm}$, //b-axis 4.10^4cm^{-1} [10a] using the following crystal data: singlet exciton lifetime $\tau_S \sim 10^{-8}$sec and diffusion length $L_s = 5.10^{-6}$cm, $S \rightarrow T$ conversion $\sim 2\%$, triplet exciton lifetime $\tau_T = 10^{-2}$sec and diffusion coefficient $D^{10b}_{T,c'} = 1.6.10^{-5}$cm^2/sec. For the steady state follows $R_{S/T} = 10$, during flash duration (15 nsec) $R_{S/T} = 500$ and during transit time (0,5 μsec) $R_{S/T} = 100$, neglecting reabsorption of fluorescence. These ratios hold only as long as the surface quenching of both types of excitons is exceeding their diffusion velocity.

Comparison of the steady state photocurrent at 347 nm at the field strengths of the transients yields a ratio of 5:1 for the currents measured with aqueous electrolyte and metal electrodes, whereas the corresponding ratio of the total charge in the transients amounts to 8:1. The inital current rise changes drastically with the two electrode types. As long as no further arguments are considered, SCF-transients, identical in shape and possibly differing in the total charge should be expected, however.

The fast rise of the current in Figure 6 is attributed to a fast charge carrier injection, including some contribution by an RC-term. A charge carrier cloud with a thickness of several lattice parameters migrates under the influence of the external field towards the counter electrode. During the duration of the flash (15 nsec) charge carriers have drifted $\sim 10^{-4}$cm into the crystal bulk, assuming $E = 10^4$ V/cm and $\mu = 1$ cm^2/V.sec. From the nearly rectangular pulse form and the steep current rise we conclude that injection of holes occurs dominantly via singlet excitons, interacting with oxygen as electron acceptor species, present in the aqueous electrode.[11] The slight increase of the current plateau in Figure 6 might indicate that appoximately 15% of the total charge originates from triplet excitons. This contribution of triplet excitons to the current, higher than expected from the crude estimate of $R_{S/T}$ may be due to different influences: (a) Reduction of $R_{S/T}$; since the diffusion length of singlet excitons is relatively short, a correction for reabsorption should predominantly increase the relative triplet exciton density. (b) Higher electron transfer efficiency of triplet as compared to singlet excitons. In earlier work[5] it has been shown that the quantum yield of charge carrier injection through triplet exciton interaction with electron ac-

ceptors like molecular oxygen in aqueous solution is of the order of unity at suffiently high O_2-concentrations. Depletion of the oxidant at the crystal surface during the flash does obviously not occur since the current plateau in Figure 6 varies linearly with the light intensity. On the other hand, with the assumption of 10^{11} singlet excitons/cm^2, being generated by 10^{12} incident photons within their diffusion length L_S, the quantum yield of hole injection via singlet excitons in the transient of Figure 6 is of the order of 10^{-2}.

From the estimate of the free charge carrier lifetime in proximity of the surface of less than 10^{-9} sec we conclude that diffusion of free charge carriers cannot effect a current rise on the time scale of 0.1 μsec. Apart from the foregoing estimate which favours a dominant role of singlet excitons in charge carrier injection, even at a metal electrode [12], the slow current rise in Figure 7 is certainly not determined by the diffusion of triplet excitons as indicated most obviously by the failure of a $t^{1/2}$-diffusion law. Moreover, a similarly shaped current transient as in Figure 7 is observed using a quinone crystal with a triplet exciton lifetime significantly shorter than the transit time [13] contrary to anthracene crystals.

Thus free charge carriers effecting a linear current rise on the time scale of the transient must have been trapped intermediately, i.e. during their lifetime in the region of the image force barrier. The trapped charge carriers can be released thermally and partly recombine at the surface, partly contribute to the current. The maximum current in Figure 7 (5.10^{-6} A/cm^2) flowing for 10 μsec would correspond to detrapping of 10^9 carriers/cm^2. A mere increase of the local trap density at the surface due to the procedure of metal deposition as trivial explanation of the different transient shapes is precluded since the slow current rise is also obtained with silver coated Mylar sheets as electrodes. In the case of incomplete charge carrier release during the transit time, e.g. by slow detrapping, the SCF transient cannot reach a constant value. Then the total charge cannot be related to that of Figure 6 in order to estimate the relative efficiency of the two electrodes. Assuming a similar quantum yield for singlet exciton charge carrier generation at both electrodes (what is somewhat supported by Ref. 12), the ratio of the total charge should be less than that observed in the steady state currents as long as the surface recombination of trapped charges is neglected.

This attribution of the slow current rise to detrapping of shallow traps is furthermore supported by the following experimental findings: Upon a few repetitions of the transient the current rise becomes gradually steeper (Figure 8a). It is also steep from the very beginning when instead of silver a gold electrode is used, the latter injecting an appreciable SCL-hole current (10^{-6}A/cm^2 at 10^4V/cm) in the dark contrary to silver which injects less than 10^{-11} A/cm^2 at the field strengths of this paper. The steep rise is associated with residual space charge and deep traps gradually occupied, the thermal release time of these traps being at least twice the transit time or longer. The steep initial rise

would in this case reflect the detrapping of a comparable small fraction of carriers which have been captured in deep traps. This detrapping can proceed either directly or by exciton interaction. The originally slow current rise, as observed in the measurement of Figure 7, can be reestablished by increasing the temperature during a dark period with the electric field applied (Figure 8b) or by the well-known techniques of optical detrapping.

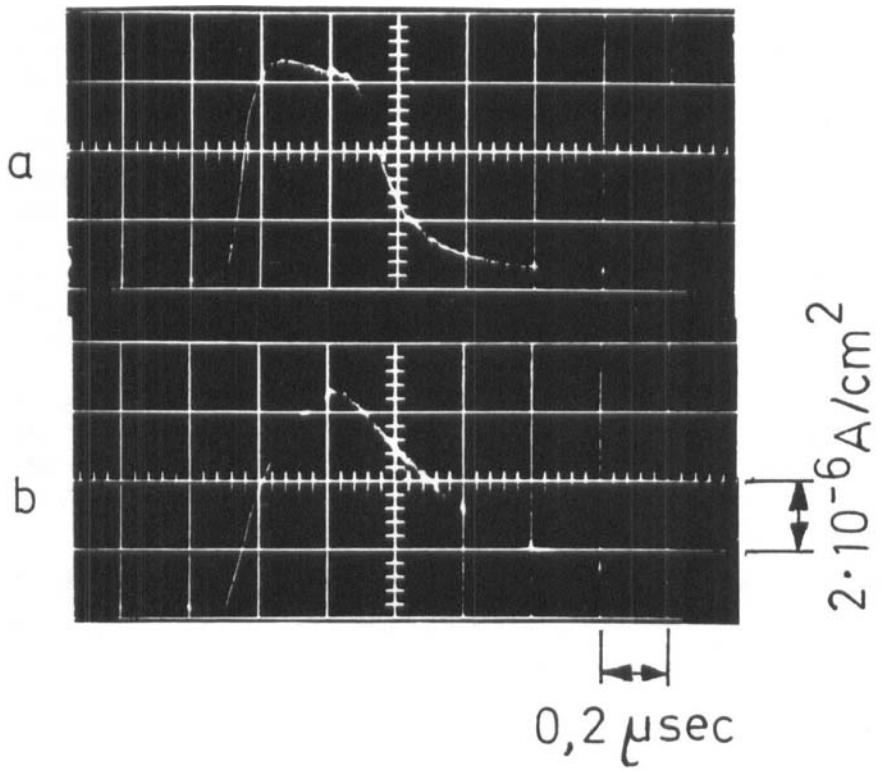

FIGURE 8 SCF-transients in anthracene crystal. Electrode, excitation, photon density and field strength as in lower trace of Figure 7. (a) transient after several flashes at 20°C. (b) transient after intermediate heating to 40°C with the electric field applied and subsequent cooling to 20°C.

CONCLUSIONS

Hole injection into anthracene crystals by exciton decay at a silver contact is determined by the action of the image force and by surface recombination of charge carriers. In the steady state experiments this gives rise to a linear current-voltage-relationship at moderately high electric fields (beyond the space charge limitation), the slope of which allows an estimate of the surface recombination velocity of 10^3 cm/sec. When the external field is comparable to the image force field, the current deflects into saturation. This behaviour is quantitatively covered by the model. In Kepler type transient experiments with a short laser flash, the current increases linearly in time until the carriers reach the back electrode. This behaviour is consistent with the following mechanism: During flash duration carriers are created, which cannot escape immediately the surface region due to the image forces. Instead they either recombine or become trapped near the surface within their lifetime. The trapped particles will be released thermally, giving rise to a diffusion current over the potential maximum which is approximately constant in time. Thus the number of carriers within the bulk of the crystal and hence the observed current increase linearly. The situation with an aqueous electrolyte is simpler since the orientation polarization of the water molecules is slower than the carrier hopping time within the crystal. The image forces are therefore negligible and consequently, the steady state current-voltage relationship shows saturation at rather low field strengths, just beyond SCL limitation. In the transient experiments as well the absence of image forces facilitates charge seperation: Immediately after their creation the charge carriers drift within the applied field and cause an nearly time independent current pulse until the transit time.

Another difference between transients with silver and aqueous electrodes is the slightly prolonged transit time in the latter case, observed for sufficiently thin crystals. This again supports the assumption that charge carriers generated at a metal electrode have to overcome an image potential barrier.

Acknowledgements

We would like to thank Professor Kallmann for stimulating discussions and critical reading of the manuscript. Financial support by the Deutsche Forschungsgemeinschaft is gratefully acknonledged.

References

1. M. E. Michel-Beyerle and R. Haberkorn, *Z.Naturf*, **27a**, 1496 (1972).
2. W. Mehl and J. M. Hale in *Advance in Electrochem. Eng.*, Vol. 6, Edited by P. Delahay (Interscience, 1967).
3. C. A. Barlow, *ibid.*
4. Review by W. Helfrich in *Physics and Chemistry of the Organic Solid State*, Vol. III, edited by D. Cox, M. M. Labes and A. Weissberger (Interscience, 1967).

5. M. E. Michel-Beyerle, F. Willig, *Chem. Phys. Lett.* 5, 28 (1970). According to the rate constant $k_1 = 10^6$ cm^4/molsec an O_2-concentration of $\sim 10^{-3}$ M/1 (in equilibrium with air) should be sufficient for the saturation current A in Figure 3 to be diffusion controlled with respect to the triplet excitons.
6. H. Kallman and M. Pope, to be published.
7. C. Bogus, *Z.Physik* 207, 281 (1968).
8. M. Pope and H. Kallmann, *Disc. Farad. Soc.* 1971, review.
9. F. Gutmann and L. E. Lyons, *Organic Semiconductors*, (J. Wiley, N.Y., 1967) and references therein.
10. (a) C. B. Clark and M. R. Phillpott, *J. Chem. Phys.* 53, 3790 (1970); (b) P. Avakian and R. E. Merrifield, *Mol. Cryst.* 5, 37 (1968).
11. D. Handel, Technische Universität, München 1970.
12. H. Kallmann, G. Vaubel and H. Bässler, *Phys. Stat. Sol.* (b) 44, 813 (1971).
13. R. Haberkorn, W. Harengel and M. E. Michel-Beyerle, *Ber. Bunsenges. Physik. Chemie*, in press.
14. J. Mort, F. W. Schmidlin and A. I. Lakatos, *J. Appl. Phys.* 42, 5761 (1971).
15. H. P. Braun, R. Haberkorn and M. E. Michel-Beyerle, *Z. Naturforsch.* (b), to be published.

APPENDIX

THE DEPENDENCE OF THE CURRENT ON THE EXTERNALLY APPLIED ELECTRIC FIELD.

In order to derive the relationship between the steady state particle current density j and the applied electric field E we solve the equation

$$j = -D\left[\frac{dn}{dx} + \frac{q}{kT} n \frac{dU}{dx}\right] \tag{A.1}$$

for the geometry indicated in Figure 4.

The coordinate x denotes distance from the contact, q the charge of the carriers, kT the thermal energy, D the diffusion constant (related through Einstein's relation with the drift mobility μ), and $n(x)$ the carrier density.

In the absence of space charge, the electric potential energy $qU(x)$ is given by

$$qU(x) = -qEx - \frac{q^2}{4\epsilon x} \quad \text{with } Eq > 0 \tag{A.2}$$

ϵ being the dielectric constant of the molecular crystal. The first term arises from a constant external electric field, and the second term is the image potential generated by the boundary at $x = 0$.

We assume that particles are created with a rate I at a distance $x = a$ of the order of the lattice constant from the interface. The relationship between the current density j and the injection rate I in this first molecular layer is given by

$$j = I - \nu\, n(a) \tag{A.3a}$$

where ν is the surface recombination velocity of the particles. For large values of x we choose the particle density to be equal to zero, i.e.

$$n(\infty) = 0 \tag{A.3b}$$

The solution of Eq. (A.1) for the boundary conditions (A.3) has the form

$$j = I \left\{ 1 + \frac{\nu}{D} \int_a^\infty \exp\left[\frac{q}{kT}\ U(x) - U(a) \right] \mathrm{d}x \right\}^{-1} \tag{A.4}$$

as derived by Kallmann and Pope[6]. An approximate solution for large a with application to CdS and amorphous Se is given in Ref. 14. This solution is, however, not applicable to molecular crystals like anthracene.

For comparison with experimental curves we introduce a change of variables in Eq. (A.4) which yields

$$j = I \frac{E}{E + \tilde{E}} \tag{A.5}$$

The new variable $\tilde{E}$ is defined by $\tilde{E} = \nu S/\mu$ with a dimensionless integral

$$S = \int_0^\infty \exp(-\zeta) \exp(s\zeta(\zeta + r)^{-1})\, \mathrm{d}\zeta \tag{A.6}$$

where $r = qEa/kT, s = q^2/4\epsilon akT$ and $\zeta = r(x/a - 1)$ (A.7)

In the low field limit when E is much smaller than the image field ($r \ll s$) the integral is easily evaluated, giving

$$E = \frac{\nu}{\mu} \exp(q^2/4\epsilon akT) \text{ for } E \ll \frac{q}{4\epsilon a^2} \tag{A.8}$$

In the high field limit, $r \gg s$, Eq. (A.6) yields

$$E = \frac{\nu}{\mu} \text{ for } E \gg q/4\epsilon a^2. \tag{A.9}$$

For arbitrary values of the applied electric field E, the integral in Eq. (A.6) can be numerically evaluated using the Gauss-Laguerre method.